Available online at www.sciencedirect.com
SCIENCE DIRECT®
Polymer 45 (2004) 1885–1893
polymer
www.elsevier.com/locate/polymer

# Poly(benzobisoxazole divinylene): synthesis, photophysical properties, and electron paramagnetic resonance studies

Peiying Guo, Shanfeng Wang[1], Pingping Wu, Zhewen Han*

*Key Laboratory for Ultrafine Materials of Ministry of Education, School of Materials Science and Engineering, East China University of Science and Technology, Shanghai 200237, China*

Received 4 November 2003; received in revised form 28 December 2003; accepted 17 January 2004

**Abstract**

A new conjugated rigid-rod polymer, poly(benzobisoxazole divinylene) (PBODV) has been synthesized and characterized using FTIR, $^1$H NMR, viscometry, wide-angle X-ray diffraction, and thermogravimetric analysis. UV absorption spectroscopy and photoluminescence spectroscopy were also used to investigate the photophysical properties of these polymers in methanesulfonic acid in detail. The results show that the introduction of *trans*-vinylene segments into the poly(benzobisoxozale)s backbone narrowed the optical bandgap of this class of polymers. The excitation and emission spectra change significantly with the concentration both in shape and the peak positions, indicating the formation of aggregates in solution. Furthermore, electronic paramagnetic resonance studies show the intrinsic paramagnetic defects in the PBODV, which can be interpreted using a soliton–antisoliton model.


*Keywords:* Polycondensation; Photophysics; Conjugated polymers

## 1. Introduction

The synthesis and processing of conjugated polymers as electronic, optoelectronic, and nonlinear optical materials have attracted considerable attention from the scientific community because of their semi-conducting and luminescent properties [1,2]. Photophysical properties of conjugated polymers are important for both understanding the nature of their excited states and the construction of electroluminescent devices. The energy gap of conjugated polymers may be modulated by changing polymer substitution or copolymer composition [3,4].

The poly(benzazole) family, shown in Scheme 1, has been studied since the early 1980s [5,6]. It includes poly(benzobisthiazole)s, poly(benzobisoxazole)s, and poly(benzimidazole)s. The rigid-rod or semi-rigid structures of these polymers bring about many advantageous physical properties such as high tensile strength, high modulus, and outstanding thermal and environmental stability. Moreover, it is well established that the benzoxazole group has a considerable chromophoric effect on the fluorescence of conjugated systems [7,8]. This class of polymers is favorably considered to be superior electron-transport and hole-blocking materials in polymer light-emitting diodes (LED) [9].

It was also reported [10] that poly(benzazole)s have significant electron paramagnetic resonance (EPR) signals and a soliton–antisoliton model was established to explain the EPR signals in such polymers. EPR studies can offer some interesting information about the origin and nature of the electrons, which is helpful to understand the electrical conductivity and paramagnetic properties.

In the earlier studies by Jenekhe and Osaheni [11], new heterocyclic polymers including poly(benzobisthiazole-2,6-diylvinylene) (PBTV), and poly(benzobisthiazole-2,6-diyl-divinylene) (PBTDV) were synthesized and characterized based on poly(*p*-phenylene benzobisthiazole) (PBZT), which has been known as a good nonlinear optical polymer. They proposed that phosphorylation increases the reactivity of the diacids in the following order: *trans*, *trans*-muconic acid > fumaric acid > oxalic acid in the process of synthesis. They also studied the photophysical properties and film processing of these polymers and found that these new polymers had smaller optical bandgap than PBZT.

* Corresponding authors. Address: Department of Polymer Science, The University of Akron, 242 McGowan Street, Apt. 6, Akron, OH 44306, USA. Tel.: +1-330-972-2158; fax: +1-862-164-233-269.
*E-mail address:* zhwhan@ecust.edu.cn (Z. Han).
[1] Department of Polymer Science, The University of Akron, OH, USA. *E-mail address:* shanfeng_wang@yahoo.com (S. Wang).

0032-3861/$ - see front matter © 2004 Elsevier Ltd. All rights reserved.
doi:10.1016/j.polymer.2004.01.027

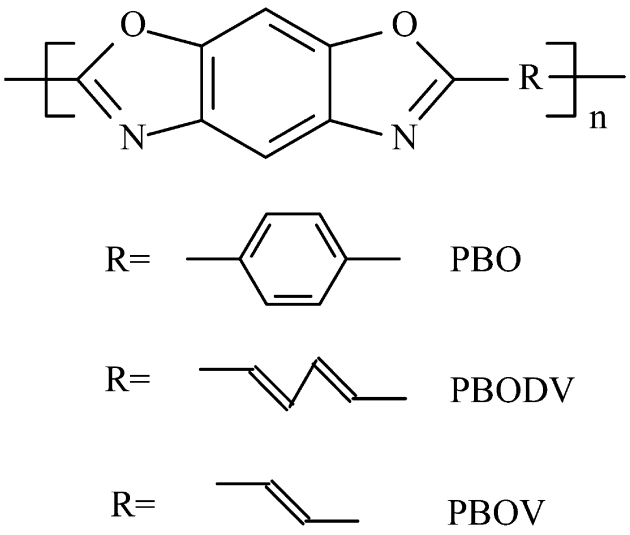


Scheme 1.

In order to extend such a scheme to another rigid-rod polymer PBO, one derivative of poly(*p*-phenylene benzobisoxazole) (PBO), poly(benzobisoxazole divinylene) (PBODV) was prepared presently in this work. Furthermore, the structure and properties of PBODV have been characterized to show a new electronic absorption spectrum, which allows the studies of structure–property relationship in this class of polymers. The chemical structure of PBODV is depicted in Scheme 1 together with another derivative of PBO, poly(benzobisoxazole-2,6-diylvinylene) (PBOV). The photophysical and paramagnetic properties of these polymers were also investigated in detail to advance the utilization of polybenzazoles in electronics.

## 2. Experimental

### 2.1. Polymer synthesis

In the synthesis of PBODV shown in Scheme 2, 2,4-diamino-1,5-benzenediol dihydrochloride (DABDO) (3.20 g, 15 mmol) was dissolved in 31.63 g of deaerated 80.8% PPA (polyphosphoric acid) in a glass reaction vessel purged with argon. After dehydrochlorination at 80 °C under vacuum, the reaction vessel was cooled down to about 50 °C, and then 2.132 g (15 mmol) of muconic acid (MA) was added together with 16.68 g of fresh $P_2O_5$. The reaction mixture was stirred for 30 min to ensure fully mixing of the monomers. The reaction temperature was raised to 80 °C and held for 6–10 h, then to 120 for 6–10 h. The highly viscous polymerization dope (brown in color) in PPA was precipitated in water and purified by extraction of the PPA with water for 2–3 days. The polymer was desiccated at 60 °C in a vacuum oven.

PBO was synthesized according to the report [12] using a similar method.

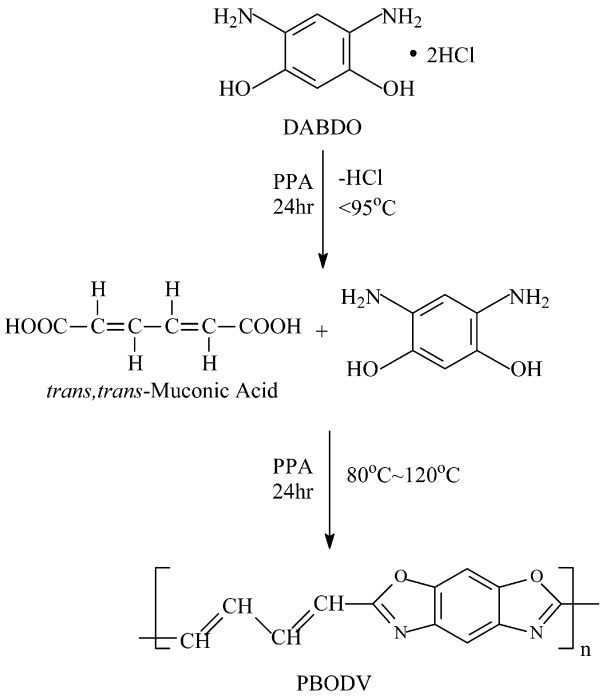


Scheme 2.

### 2.2. Characterization

Intrinsic viscosities [$\eta$] of all the polymers were measured in methanesulfonic acid (MSA) at 30 °C using a modified Ubbelohde capillary viscometer [13]. MSA was obtained from Sigma-Aldrich Chemical Co. Thermogravimetric analysis (TGA) was done using a Du Pont Model 951 thermal analyst. The TGA data were obtained in flowing nitrogen at a heating rate of 10 °C/min. Fourier transform infrared (FTIR) spectra were taken at room temperature using a Nicolet Magna-IR 550 FTIR spectrometer. Free-standing films were used for obtaining the IR spectra of PBODV. The $^1$H NMR spectra were taken at 500 MHz using a Bruker DMX-500 instrument. Polymer solutions for NMR measurement were prepared in a drybox using deuterated sulfuric acid as the solvent.

Optical absorption spectra of the polymer thin films were recorded on a VARIAN Cary 500 UV–vis–near-IR spectrophotometer. Thin films of good optical quality were prepared by spin coating of Lewis acid-based complexes in nitromethane/$AlCl_3$ solution onto glass substrates, followed by decomplexation in deionized water [11]. Optical absorption spectra of the polymer solutions obtained with a UNICO UV-2102 PCS spectrophotometer. Photoluminescence spectra were recorded on a VARIAN Cary Eclipse fluorescence spectrophotometer at room temperature.

Wide-angle X-ray diffraction (WAXD) of PBO and PBODV obtained on a Rigaku D/max-rB automated powder diffractometer. The instrument was set up with a Cu Kα ($\lambda = 0.154056$ nm) X-ray source operating at 40 kV and 100 mA. The $2\theta$ scan range was set to be 3–50°.

A HITACHI ER-200D EPR spectrometer was used in the EPR studies. The resonance frequency was 9.7735 GHz and the modulating frequency was 100 kHz. Quantitative EPR measurements were monitored by comparison to a ruby standard with the spin concentration $N_s$ of about $2.6 \times 10^{18}$ spins/g.

## 3. Results and discussion

### 3.1. Synthesis and microstructure

Similar to the preparation of PBO, the synthesis of PBODV is a process of the condensation polymerization of a diacid and DABDO to form the benzobisoxazole ring in a polymer backbone as depicted in Scheme 2. In the process of synthesis, PPA also played a key role of catalyst besides the medium of polymerization. The macromolecule chain growth relied on the phosphorylation of both amine and acid groups, namely the activation of these two functional groups, and the phosphorylation of aliphatic acids made the functional groups very reactive even at low temperature. Compared with PBO (180 °C), PBODV had a much lower polymerization temperature (120 °C), which implies that *trans*, *trans*-muconic acid was much easier to be activated than terephthalic acid.

The polymer structures were established primarily by FTIR and $^1$H NMR. Fig. 1 shows a comparison of the FTIR spectra of PBODV and PBO. As can be seen in Fig. 1, there is no strong amide band (–NHC(O)–) at 1670 cm$^{-1}$, indicating that complete closure of the oxazole rings in the polymerization has been achieved [11]. The characteristic peaks of these two polymers in FTIR spectra are listed in Table 1.

The $^1$H NMR spectrum of PBODV was obtained in deuterated sulfuric acid. Fig. 2 shows the $^1$H NMR spectrum of PBODV and its assignment. The number of protons corresponding to each resonance is in good agreement with the proposed structure. $^1$H NMR (deuterated sulfuric acid, ppm): $\delta = 8.1, 8.9, 9.1, 9.3$. The $^1$H NMR result here can be considered as a good characterization for polybenzazoles together with our previous $^1$H and $^{13}$C NMR characterizations of PBO model compound and PBO film [14].

### 3.2. Intrinsic viscosity, thermal stability, and morphology

The intrinsic viscosities of PBO and PBODV in MSA at 30 °C are 24.5 and 5.7 dl/g, respectively. The weight-average molecular weight of PBO is 26,000 g mol$^{-1}$ estimated using Mark–Houwink equation [12]. Although there is no established Mark–Houwink equation for PBODV, a rough estimation of the molecular weight can be made from the intrinsic viscosity data using the equations for PBO and a semi-rigid polymer poly(2,5-benzoxazole) (ABPBO) [12]. The intrinsic viscosity of 5.7 dl/g for PBODV can be translated to a weight-average molecular weight of 11,600 in the lower limit and 42,300 in the upper limit. Fig. 3 shows the TGA thermograms of PBO and PBODV. It can be observed from Fig. 3 that the thermal stability of PBODV is lower than that of PBO (the decomposition temperature is around 675 °C) as expected, since aromatic ring is much more stable than aliphatic

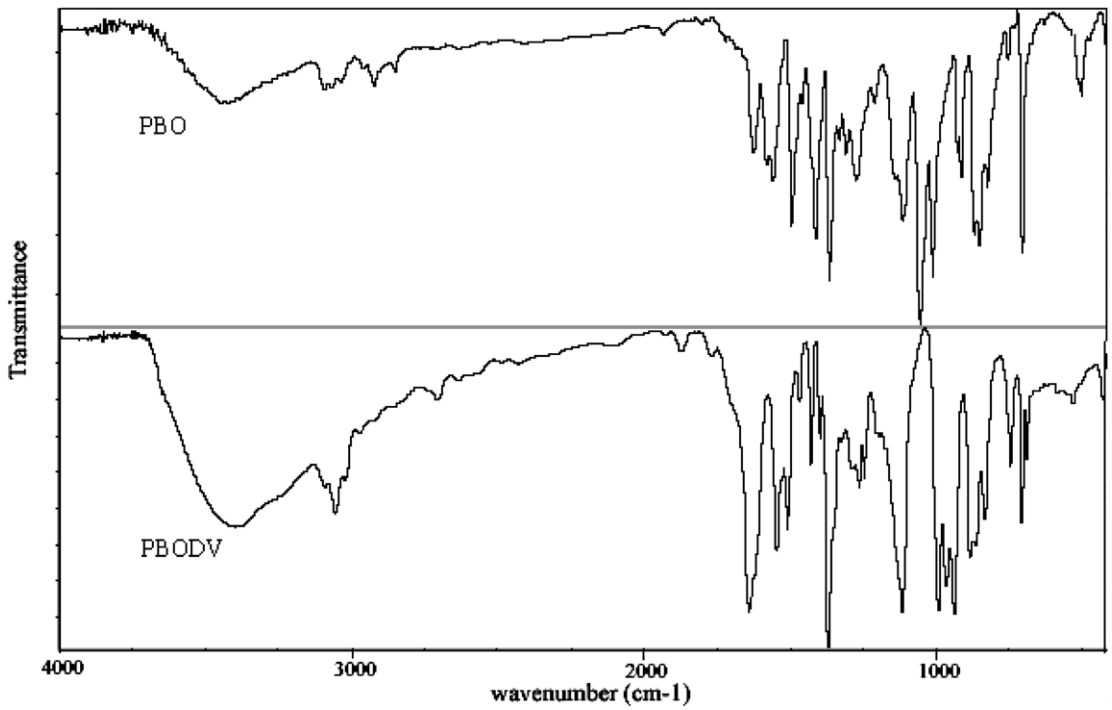


Fig. 1. FTIR spectra of PBO and PBODV.

Table 1
Summary of IR spectra of polymers

| Assignment | Frequency ($cm^{-1}$) | |
|---|---|---|
| | PBODV | PBO |
| Asym. C=C stretch | 1624 | |
| Hetero-ring stretch (vs) | 1508 | 1498 |
| 1,4-$C_6H_4$ | | 1410 |
| Hetero-ring stretch (vs) | 1365 | 1363 |
| *trans*-vinylene | 1053 | |
| Hetero-ring 'breathing' (vs) | 1113 | 1113 |
| 1,4-$C_6H_4$ | | 1055 |
| *trans*-vinylene | 962 | |
| 1,2,4,5-$C_6H_2$(s) | 864 | 868 |
| Hetero-ring out-of-plane def. | 704 | 704 |

moieties [11]. Still, PBODV has reasonably good thermal stability. The decomposition in nitrogen starts at ~490 °C, which is slightly higher than the decomposition temperature of PBTDV (~460 °C) synthesized by Osaheni and Jenekhe [11]. When temperature arrived 700 °C, there was still around 60% residual left. The slight weight loss between 200 and 260 °C can be attributed to the residual PPA left in polymer during polymerization.

The morphology of the polymers was investigated by WAXD. The result in Fig. 4 shows the radial profiles along the equatorial direction corresponding to the orientation of polymer films. The X-ray powder diffraction pattern of PBODV in Fig. 4 showed two broad peaks similar to the diffraction pattern of PBO, the two major peaks of PBODV films offer an indication of their microstructure. The first peak around $2\theta = 16°$ corresponds to the side-to-side

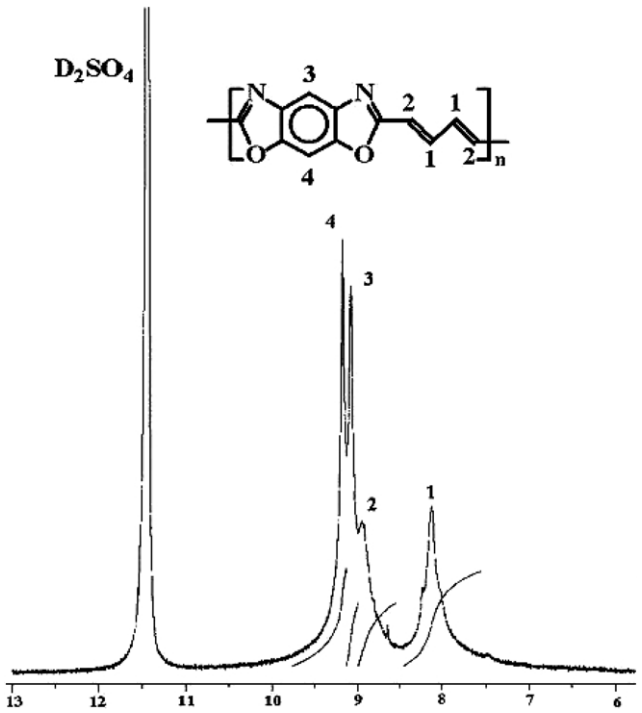


Fig. 2. $^1$H NMR spectra of PBODV.

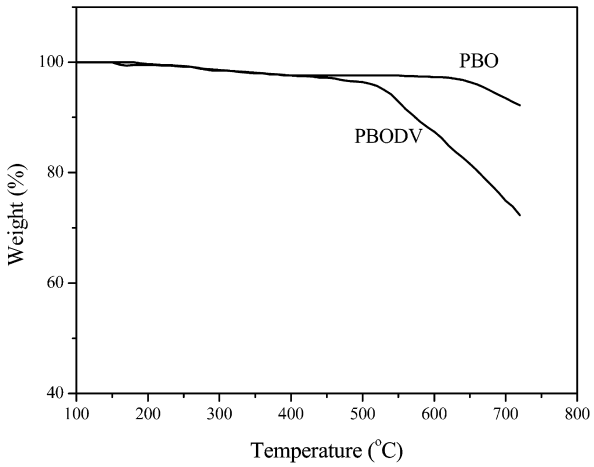


Fig. 3. TGA thermograms of PBO and PBODV.

distance between rod molecular chains of poly(benzobisoxazole)s. This broad diffraction peak in PBODV is at *d*-spacing of 0.57 nm, while in PBO is at *d*-spacing of 0.55 nm, which corresponds to (200) plane [15]. The second peak around $2\theta = 26°$ corresponds to the face-to-face distance between two neighboring chains. The peaks for PBO and PBODV here correspond to a *d*-spacing of 0.34 nm. The results indicate that the chain packing in the divinylene polymer PBODV are similar to that in PBO. However, the main equatorial peaks of the PBODV films are not as well defined as those of PBO and there is a continuous scattering between the (200) and (010) reflections, which gives an indication of a poorly developed lateral order of the PBODV chains.

### 3.3. Photophysical properties

Fig. 5 shows the optical absorption spectra of the divinylene-linked polymer PBODV and PBO solution in MSA along with their thin film spectra. The concentration of the polymers in MSA is 0.0044 g/dl, corresponding to

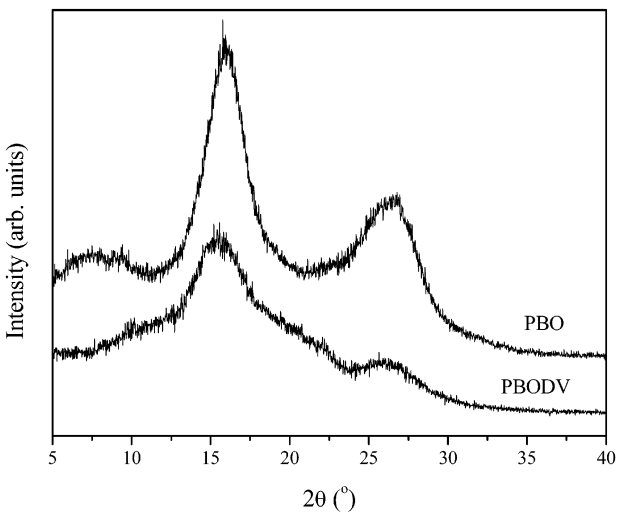


Fig. 4. Wide angle X-ray diffraction curves for PBO and PBODV.

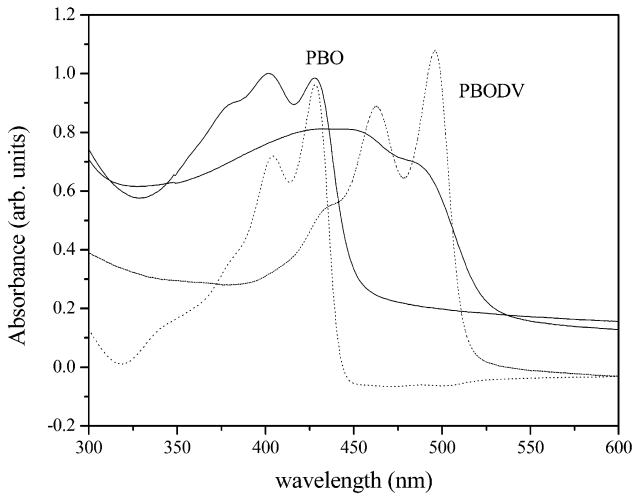


Fig. 5. Absorption spectra of PBO and PBODV in methanesulfonic acid solutions (dotted curves) at the concentration of 0.0044 g/dl and thin films (solid curves).

$2.1 \times 10^{-4}$ M. Absorption data of polymers considered here were listed in Table 2.

Though the optical absorption spectra of PBO and PBODV are very similar, it is evident that the main difference is that the spectrum of the *p*-phenylene linked PBO ($\lambda_{max} = 429$ nm) is red shifted to that of the divinylene linked PBODV ($\lambda_{max} = 496$ nm), resulting in an optical bandgap that is 0.35 eV lower than that of PBO ($E_g = 2.76$ eV) [16]. The intermediate peak positions for PBO and PBODV are 405 and 463 nm, respectively. It has been reported [17] that the introduction of vinylene into conjugated polymers can reduce the optical bandgap ($E_g$), just as the polyphenylene has an $E_g$ of 2.8 eV and the polyacetylene has an $E_g$ of 1.5 eV [18]. Fig. 5 also shows that the bandwidth of the $\pi-\pi^*$ transition of PBODV is wider than that of PBO. These results are expected because the extent of $\pi$-delocalization over the repeating units and $\pi$-electron conjugation of PBODV are greater than those of PBO, which are also in agreement with the earlier comparison for PBTDV and PBZT [11].

It should be noted that the spectra of thin films are similar to those of polymer solutions except they are more featureless. Meanwhile, the bandwidth and optical absorption threshold of polymer solid thin films are broadened. The implication of this phenomenon is that the interchain interactions of solid-state polymers are larger than that of polymer solutions. However, it can be seen that the trend in the $\lambda_{max}$ or optical bandgap of solid-state spectra is similar to that of solution spectra because of the intrinsic electronic properties of the polymers which are mainly affected by intramolecular interactions instead of intermolecular interactions.

Table 2
Absorption, excitation and emission wavelength of polymers considered herein

| | PBO | | PBODV | |
|---|---|---|---|---|
| | Solution | Film | Solution | Film |
| $\lambda_1$ (nm) | 405 | 402 | 463 | 445 |
| $\lambda_2$ (nm) | 429 | 428 | 496 | 492 |
| Ex[a] (nm) | 433 | | 490 | |
| $Em_1$[b] (nm) | 440 | | 509 | |
| $Em_2$[b] (nm) | 466 | | 541 | |

[a] Excitation wavelength.
[b] Emission wavelength.

Fig. 6 shows the photoluminescence spectra of PBO and PBODV in MSA at the concentration of 0.0044 g/dl. Although the excitation and emission spectra of different polymers display striking changes in wavelength of the peak, the excitation and emission profiles of PBODV have similar characteristics to PBO and both exhibit discrete vibronic features. The peak positions are also listed in Table 2. Similar to absorption spectra, excitation spectra and emission spectra also show a red shift of the peaks from PBO to PBODV. The difference in emission peaks of two polymers offers a possible method to get copolymers with PBO and PBODV to achieve spectral tunability between the bandgap energy $E_g$ of 2.41 and 2.76 eV.

### 3.4. Formation of aggregates in PBODV in MSA

The photoluminescence spectra of PBODV in MSA are shown in Fig. 7 at concentrations ranging from 0.0044 to 0.088 g/dl, corresponding to $2.1 \times 10^{-4}$ and $4.2 \times 10^{-3}$ M, respectively. The photoluminescence spectra of PBO in MSA at various concentrations have been studied in detail by our laboratory previously [19]. From Fig. 7, the progressive trends in excitation spectra and emission spectra for PBODV in MSA similar to the previous report on PBO in MSA can be observed. Firstly, the line shape of excitation spectra changes dramatically with concentration, which was

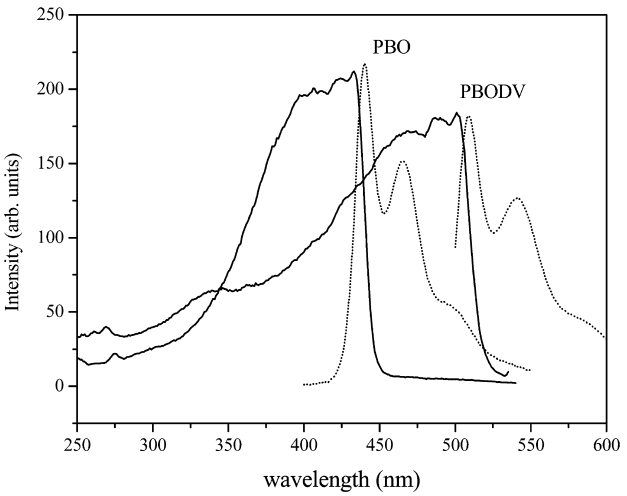


Fig. 6. Photoluminescence excitation (solid curves, monitoring wavelengths are 440 and 510 nm for PBO and PBODV, respectively) and emission (dotted curves) spectra of PBO and PBODV in MSA at the concentration of 0.0044 g/dl excited at 430 and 490 nm, respectively.

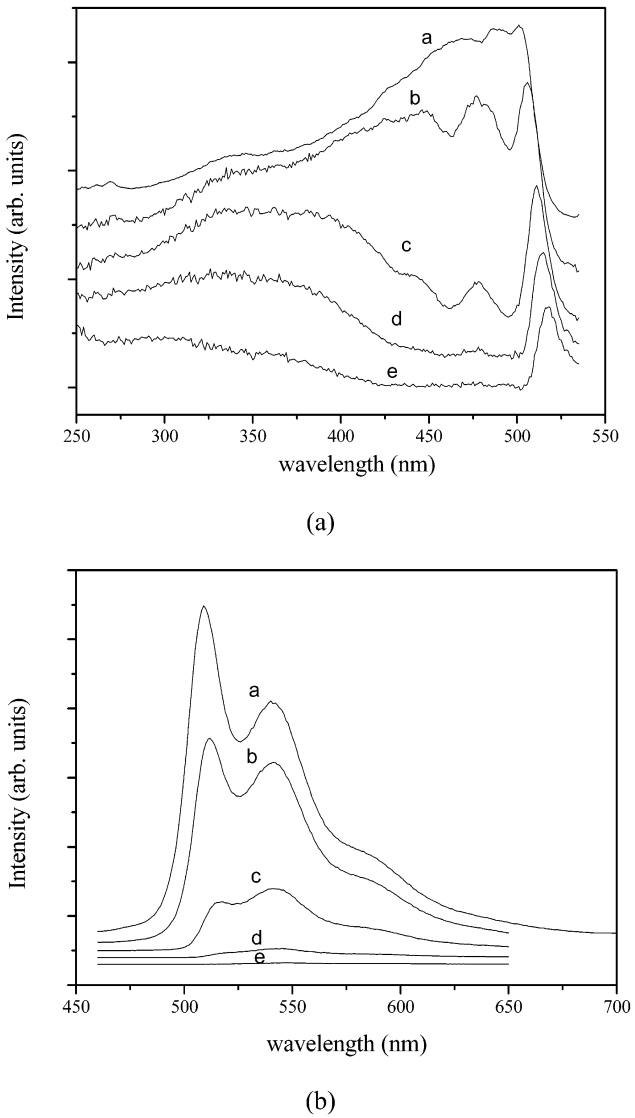


Fig. 7. Photoluminescence ((a) excitation, (b) emission) spectra of PBODV in MSA (a, b, c, d, e: 0.0044, 0.0088, 0.022, 0.044, and 0.088 g/dl, respectively) excited at 496 nm, the monitoring wavelength for obtaining excitation spectra is 510 nm.

also reported for PBO solutions [19]. Secondly, the emission peak has some striking changes, for examples, the emission intensity decreases and the spectrum becomes broad and featureless gradually with increasing concentration.

In Fig. 7(a), it can be observed initially a broad, strong excitation peak in the spectrum of very dilute solution at the concentration of 0.0044 g/dl. This broad, strong peak is formed by three components and it splits progressively to three separate peaks at higher concentrations. One component is at the longer wavelength and it is red shifted slightly with the concentration from 501 to 518 nm for PBODV (compared with the redshift from 430 to 460 nm for PBO [19]). When the concentration increases, this component becomes more conspicuous. The second component around 478 nm was not reported for PBO [19]. The position of this peak does not change much, but it disappears quickly with increasing concentration. The third component is at the shorter wavelength; it separates from the other components and is blue shifted from 446 nm at 0.0088 g/dl to 300 nm at 0.088 g/dl. The intensity of these three peaks all diminishes with increasing concentration, but the first peak is still discernable when another two peaks almost completely disappear due to the self-quenching effect and internal filtration at high concentrations.

The emission peaks of PBODV shown in Fig. 7(b) can be divided into two groups. The first group appears at about 510 nm, the second appears at about 540 nm. They are all red shifted compared to the first two peaks of PBO [19]. The emission spectra of polymers changes dramatically with concentration. At the lowest concentration (0.0044 g/dl) in this study, the emission spectrum contains two peaks and shows a well-resolved vibronic stucture and it is symmetric with the absorption spectra. When the concentration increases to 0.0088 g/dl and the broad peak begins to show the tendency to split in the excitation spectrum, the intensity of the two peaks and their ratio decreases greatly although the corresponding emission spectrum is still similar to that of 0.0044 g/dl. With further increase in concentration, the change in the line shape of emission spectra begins to aggravate. The first peak progressivly diminishes to a shoulder and the second peak becomes dominant in the emission spectra; the ratio of the first peak intensity and the second peak intensity decreases from 1.44 at 0.0044 g/dl to 0.78 at 0.022 g/dl for PBODV. When the concentration increases to 0.088 g/dl, the first peak almost disappears when internal filtration effect begins to perturb the emission spectrum.

Other than the measurement artifact of internal filtration effect, another important phenomenon is the fluorescence self-quenching of polymer solutions with the increasing of concentration. The self-quenching is a result of the combined effect of many physical and chemical processes. At high concentrations, the excited molecules may get more probability to dissipate energy by other means, for example, forming aggregation or deactivation process in which the energy transfer results in the formation of excitation state. The self-quenching of PBODV are more obvious than that of PBO [19]. We can hardly see fluorescence emission at concentration of 0.044 g/dl for PBODV, while a weak fluorescence emission can still be observed for PBO at concentration of 0.12 g/dl. This phenomenon can also be attributed to that PBODV have greater $\pi$-delocalization over the repeating units, which makes PBODV chains have higher intermolecular interactions and easier to form aggregation than PBO. Here, the aggregation is a rather broad term including the physical aggregate and excimer proposed by Jenekhe for solid PBZT films [20]. However, our detailed experiments have provided strong evidence of aggregate formation of PBO chains in MSA [19].

There are many interpretation on the origin of the large apparent Stokes shift between the emission and absorption

maxima ($\Delta\lambda_{max}$) in π-conjugated polymers (~0.3–0.7 eV). Rauscher and co-workers [21] suggested that this was a result of excitation migration and transfer to the lowest π–π* excitation energy chromophore from which emission occurs. However, excimer emission was proposed to account for the large $\Delta\lambda_{max}$ in conjugated polymers and rod–coil copolymers [22]. Stokes shift reflects the structural relaxation. In our polymers, Stokes shift may have two origins [23]. One is that emission occurs from the same segments when they assume a more co-planar conformation if the time allows. Another origin is that emission occurs from ring rotation on the different segments without being hindered. For convenience, we use excitation spectra to substitute absorption spectra. As shown in Fig. 7, in the most dilute polymer/MSA solution the Stokes shift is rather small. It is only 12.2 nm for PBO [19] and 18.9 nm for PBODV, reflecting the rigid geometry of the conjugated main chain ribbon [24]. Meanwhile we can see the Stokes shift increases with the concentration, indicating the aggregation of polymer chains. Our group previously reported [19] that the intermolecular interactions become stronger at higher concentrations and aggregates can be formed by two or more neighboring chains before the chromophores are excited. So this intermolecular interaction is responsible for the different photochemical behavior of these polymer solutions at different concentrations.

### 3.5. EPR studies of poly(benzobisoxazole)s

The essence of EPR is the transition of unpaired-electron of paramagnetic ion or electron-hole center on the paramagnetic state between spin substrates. As shown in Fig. 8, it is evident that the poly(benzobisoxazole)s represented here are paramagnetic and the spin concentrations are sufficiently high to suggest that the paramagnetic centers are intrinsic. As reported previously [10], there is no EPR signal in DABDO dihydrochloride, one of the monomers for preparing poly(benzobisoxazole)s as shown in Scheme 2 while the model compounds with limited number of conjugation have obvious EPR signals. As we can see from Fig. 8, the typical EPR signal of the poly(benzobisoxazole)s is a singlet without resolved hyperfine splitting, thus no direct information about the nature of the radical species can be obtained from the EPR spectrum.

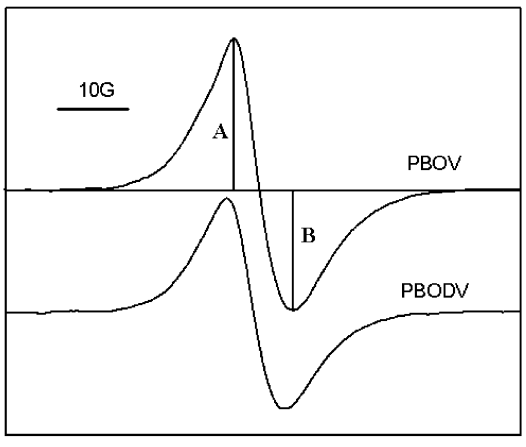


Fig. 8. EPR spectra of PBOV and PBODV, as-received (Gain, $1 \times 10^5$).

In the previous report [10], we ascribed the EPR signals in polybenzazoles to the existence of soliton and antisoliton, which is well accepted as the origin of EPR signal in conjugated polymers. Dalton et al. [25] also gave a proper explanation for the EPR signals, they thought the paramagnetic center in conjugated polymers, i.e. unpaired electron is not expected to be localized on one atom but rather is anticipated to exist in a delocalized molecular orbital (MO) as a linear combination of atomic orbital (LCAO). As to PBO, the phenyl ring or heteroring in molecule chain has two different resonance structures including benzenoid form and quinoid form and these two structures are not degenerate. A neutral defect in this case corresponds to the boundary between benzenoid and quinoid structures. Because the two resonance structures are not degenerate, defects in the poly(benzazole)s must exist in pairs: soliton–antisoliton, as illustrated in Fig. 9. Similar model can be constructed for PBOV.

PBODV has phenyl ring or heteroring and *trans*-vinylene segments at the same time. As to conjugated polymers with degenerate structures, such as *trans*-PA, the EPR spectra of the undoped and doped polymers can be rationalized in terms of the soliton defect model [26]. But there are not enough continuous *trans*-vinylene segments in PBODV chain, therefore the defect on *trans*-vinylene has to appear together with the nondegenerate structure on heteroring as illustrated also in Fig. 9.

The main results of the EPR study, including electron Zeeman *g*-factor, peak-to-peak line width $\Delta H_{pp}$ and asymmetry parameter *A*/*B* defined by the ratio the left peak height *A* and right peak height *B*, and spin concentration $N_s$ are summarized in Table 3. It should be noted that the two EPR quantitative measurements were performed on different spectrometers with different standards (a ruby standard presently and a diamond standard in previous paper [10]). The spin concentrations obtained for rod–coil copolymers are much larger than the values reported previously for PBO and copolymers PBO-ABPBO [10] by two to three orders in magnitude. More measurements should be done for verifying the $N_s$ values.

Table 3
EPR parameters of the samples considered here at room temperature

| Parameter | PBO | PBOV | PBODV |
|---|---|---|---|
| *g* | 2.0041 | 2.0029 | 2.0036 |
| $\Delta H_{pp}$ | 8.0 | 8.5 | 8.1 |
| *A*/*B* | 1.28 | 1.27 | 1.19 |
| $N_s$ ($\times 10^{15}$ spins/g) | 1.1[a] | 645 | 891 |

[a] The samples were monitored by comparison to a diamond standard [10].

PBO

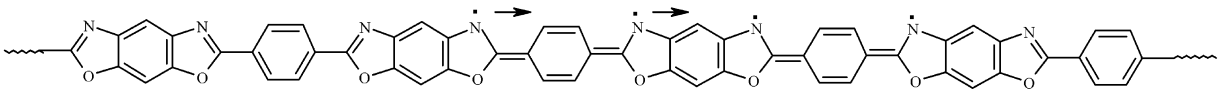

PBOV

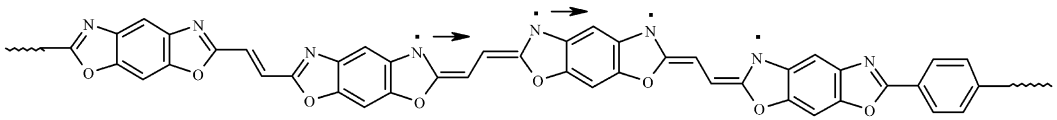

PBODV

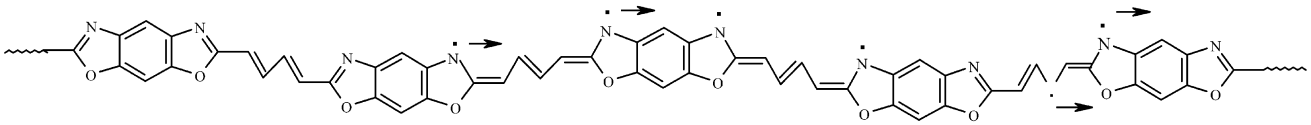

Fig. 9. Schematic representations of hypothetical soliton–antisoliton in PBO, PBODV and PBOV.

Careful *g*-factor determination was made on each of the polymers under investigation. The average *g*-values for the as-received poly(benzobisoxazole)s vary from 2.0029 to 2.0050, which is in marked contrast to a typical isotropic *g*-value of, 2.0023 observed for *trans*-PA, a *g*-value that is essentially equal to the free electron value. Any radical localized on or near a heteroatom, such as oxygen in carboxylic species or nitrogen in pyridines, has a *g*-value shift [27] of at least $10^{-3}$.

The linewidth indicates the degree of delocalization of unpaired electrons by motion, and/or by exchange. The narrower is the linewidth, the greater is the delocalization on the conjugated polymer chain. The linewidths of EPR spectra, $\Delta H_{pp}$, for the poly(benzobisoxazole)s range from 8.0 to 8.5 G approximately. Compared with 1.46 G for *trans*-PA [28] and 0.67 G for poly(thiophene) [29], the $\Delta H_{pp}$ for heteroatom-centered conjugated polymers such as poly(benzobisoxazole)s and poly(phenylene sulfide) [30] are rather large. This phenomenon can be attributed to the reason that oxygen or sulfur is not expected to participate in the π-conjugation in addition to that electron transport through nitrogen is predicted to be somewhat retarded relative to carbon [31]. The evidence from X-ray and electron diffraction, in addition to the studies of polypyrrole by Scott et al. [32], implies a system which has a considerable amount of disorder also leads to the possibility of inhomogeneous broadening through a distribution of *g*-values.

From Table 3, we can see that the poly(benzobisoxazole) films show a slight asymmetry, the *A*/*B* ratio ranges from 1.19 to 1.28. Our experiments of the heat treatment effect on the EPR of poly(benzazole)s [10] suggested that the trace amount of phosphoric acid in the as-received poly(benzazole)s results in the asymmetric EPR lines with *A*/*B* ratios of more than 1.0.

## 4. Conclusions

We have synthesized, characterized a new divinylene-linked conjugated polymer, PBODV, which is a potential material for the electronic, optoelectronic, and nonlinear optical applications. We also studied the photophysical properties of this polymer, including thin film on the glass substrates and solutions with MSA. The absorption and emission peaks for PBODV are red shifted compared with those of PBO, offering a possibility to get spectral tunability by synthesizing copolymers using PBO and PBODV. The excitation and emission spectra change significantly with concentration both in shape and the peak positions, which suggests the formation of aggregation in solutions. EPR studies of the paramagnetic defect in the poly(benzobisoxozale)s supply detailed paramagnetic properties of the new materials and a new soliton–antisoliton model involving the defects on both hetero-ring or phenyl ring and *trans*-vinylene segments was constructed to interpret the intrinsic paramagnetic signal of PBODV, which is different from the models constructed for PBO previously and PBOV.

## Acknowledgements

This research was supported by 863 project of national science and technology department of China. The number of financial item is 2002AA305109.

## References


[1] Burroughes JH, Bradley DDC, Brown AR, Marks RN, Mackay K, Friend RH, Burns PL, Holmes AB. Nature (London) 1990;347: 539–41.

[2] Skotheim TA, editor. Handbook of conducting polymer, vol. 2. New York: Marcel Dekker; 1986.

[3] Burn PL, Holmes AB, Kraft A, Bradley DDC, Brown AR, Friend RH, Gymer RW. Nature (London) 1992;356:47–9.

[4] Burn PL, Kraft A, Derek R, Bradley DDC, Brown AR, Friend RH, Gymer RW, Holmes AB, Jackson RW. J Am Chem Soc 1993;115: 10117–24.

[5] Wolfe JF, Arnold FE. Macromolecules 1981;14(4):909–15.

[6] Wolfe JF, Loo BH, Arnold FE. Macromolecules 1981;14(4):915–20.

[7] Reiser A, Leyshon LJ, Saunders D, Mijovic MV, Bright A, Bogie J. J Am Chem Soc 1972;94:2414–25.

[8] So YH, Zaleski JM, Murlick C, Ellaboudy A. Macromolecules 1996; 29:2783–95.

[9] Alam MM, Jenekhe SA. Chem Mater 2002;14:4775–80.

[10] Wang SF, Wu PP, Han ZW. Polymer 2001;42:217–26.

[11] Jenekhe SA, Osaheni JA. Chem Mater 1992;4:1282–90.

[12] Wolfe JF, Mark HF, Koschmitz JI, 2nd ed. Encyclopedia of polymer science and technology, vol. 11. New York: Wliey; 1998.

[13] Wang SF, Bao GB, Wu PP, Han ZW. Eur Polym J 2000;36:1843–52.

[14] Wu PP, Zhang X, Han ZW. Funct Polym 1992;5(3):169–74.

[15] Fratini AV, Lenhert PG, Resch TJ. Mater Res Soc Symp Proc 1989; 134:431–45.

[16] Jenekhe SA, Osaheni JA, Meth JS, Vanherzeale H. Chem Mater 1992; 4(3):683–7.

[17] Houlding VH, Nahata A, Yardley JT. Chem Mater 1990;2(2):169–72.

[18] Eckhardt H, Shacklette LW, Jen KY, Elsenbaumer RL. J Chem Phys 1989;91:1301.

[19] Wang SF, Wu PP, Han ZW. Macromolecules 2003;36:4567–76.

[20] Jenekhe SA, Osaheni JA. Science 1994;265:765–8.

[21] Rauscher L, Bassler H, Bradley DDC. Phys Rev B 1990;42:9830–6.

[22] Osaheni JA, Jenekhe SA. J Am Chem Soc 1995;117:7389–98.

[23] Bredas JL, Jerome C, Heeger AJ. Adv Mater 1996;8:447–52.

[24] Lemmer U, Heun S, Mahrt RF, Scherf U, Hopmeier M, Siegner U, Gobel EO, Mullen K, Bassler H. Chem Phys Lett 1995;240:373–8.

[25] Dalton LR, Thomson J, Nalwa HS. Polymer 1987;28(4):543–52.

[26] (a) Su WP, Schieffer JR, Heeger AJ. Phys Rev Lett 1979;42(25): 1698–701. (b) Su WP, Schieffer JR, Heeger AJ. Phys Rev B 1980; 22(4):2099–111.

[27] Carrington A, McLachlan AD. Introduction to magnetic resonance. London: Chapman and Hall; 1967.

[28] Bernier P, Rolland M, Linaya C. Polymer 1980;21(1):7–8.

[29] Tourillon G, Gourier D, Garnier P. J Phys Chem 1984;88(6):1049–51.

[30] Kispert LD, Files LA, Frommer JE, Shacklette LW, Chance RR. J Chem Phys 1983;78(8):4858–61.

[31] Forner W, Seel M, Ladik J. J Chem Phys 1986;84(10):5910–8.

[32] Scott JC, Pfluger P, Krounbi MT, Street GB. Phys Rev B 1983;28(4): 2140–5.